Received: 21 April 2019 | Revised: 23 September 2019 | Accepted: 9 October 2019

DOI: 10.1002/ajmg.c.31751

RESEARCH REVIEW

AMERICAN JOURNAL OF medical genetics PART C Seminars in Medical Genetics

WILEY

EML1-associated brain overgrowth syndrome with ribbon-like heterotopia

Renske Oegema[1] | George McGillivray[2] | Richard Leventer[3,4] | Anne-Gaëlle Le Moing[5] | Nadia Bahi-Buisson[6,7,8] | Angela Barnicoat[9] | Simone Mandelstam[10,11] | David Francis[2] | Fiona Francis[12,13,14] | Grazia M. S. Mancini[15] | Sanne Savelberg[1] | Gijs van Haaften[1] | Kshitij Mankad[16] | Maarten H. Lequin[17]

[1]Department of Genetics, University Medical Center Utrecht, Utrecht, The Netherlands

[2]Victorian Clinical Genetics Services, Murdoch Children's Research Institute, Royal Children's Hospital, Melbourne, Australia

[3]Department of Neurology, Royal Children's Hospital, Murdoch Children's Research Institute and University of Melbourne Department of Pediatrics, Melbourne, Australia

[4]Department of Pediatrics, University of Melbourne, Melbourne, Australia

[5]Department of Child Neurology, CHU Amiens, Paris, France

[6]Université Paris Descartes, Sorbonne Paris Cités, Paris, France

[7]Embryology and genetics of congenital malformations, Institut Imagine-INSERM, Paris, France

[8]Pediatric Neurology, Necker Enfants Malades Hospital, Assistance Publique-Hôpitaux de Paris, Paris, France

[9]Department of Clinical Genetics, Great Ormond Street Hospital, London, UK

[10]Royal Children's Hospital, Department of Pediatrics, University of Melbourne, Murdoch Children's Research Institute, Melbourne, Australia

[11]Royal Children's Hospital, Department of Radiology, University of Melbourne, Murdoch Children's Research Institute, Melbourne, Australia

[12]INSERM U 1270, Paris, France

[13]Sorbonne Université, UMR-S 1270, Paris, France

[14]Institut du Fer à Moulin, Paris, France

[15]Department of Clinical Genetics, Erasmus MC University Medical Center, Rotterdam, The Netherlands

[16]Department of Radiology, Great Ormond Street Hospital, London, UK

[17]Department of Radiology, University Medical Center Utrecht, Utrecht, The Netherlands

Correspondence
Renske Oegema, Department of Genetics, University Medical Center Utrecht, Utrecht, The Netherlands.
Email: r.oegema@umcutrecht.nl

Maarten H. Lequin, Department of Radiology, University Medical Center Utrecht, Utrecht, The Netherlands.
Email: m.h.lequin@umcutrecht.nl

Funding information
supported by Inserm, Centre national de la recherche scientifique (CNRS), Sorbonne Université, the JTC 2015 Neurodevelopmental Disorders affiliated with the ANR (for

Abstract

EML1 encodes the protein Echinoderm microtubule-associated protein-like 1 or EMAP-1 that binds to the microtubule complex. Mutations in this gene resulting in complex brain malformations have only recently been published with limited clinical descriptions. We provide further clinical and imaging details on three previously published families, and describe two novel unrelated individuals with a homozygous partial *EML1* deletion and a homozygous missense variant c.760G>A, p.(Val254Met), respectively. From review of the clinical and imaging data of eight individuals from five families with biallelic *EML1* variants, a very consistent imaging phenotype emerges. The clinical syndrome is characterized by mainly neurological features

NEURON8-Full- 815-006 STEM-MCD, to FF, NBB) and the Fondation Maladies Rares/ Phenomin (project IR4995, FF).

including severe developmental delay, drug-resistant seizures and visual impairment. On brain imaging there is megalencephaly with a characteristic ribbon-like subcortical heterotopia combined with partial or complete callosal agenesis and an overlying polymicrogyria-like cortical malformation. Several of its features can be recognized on prenatal imaging especially the abnormaly formed lateral ventricles, hydrocephalus (in half of the cases) and suspicion of a neuronal migration disorder. In conclusion, biallelic *EML1* disease-causing variants cause a highly specific pattern of congenital brain malformations, severe developmental delay, seizures and visual impairment.

KEYWORDS

EML1, gray matter heterotopia, hydrocephalus, megalencephaly, polymicrogyria, ribbon-like heterotopia

1 | INTRODUCTION

Gray matter heterotopia are genetically heterogeneous malformations of cortical development (MCD) in which neurons fails to reach the cortical plate during migration. Most commonly, periventricular nodular heterotopia (PNH) or subcortical band heterotopia (SBH) are observed. However, other rarer forms of gray matter heterotopia exist.

In 2014, mutations in *EML1* (Echinoderm microtubule-associated protein-like 1 or EMAP-1, MIM *602033) were first described causing a novel syndrome with ribbon-like subcortical heterotopia in five individuals from two families (Kielar et al., 2014). A sixth affected individual was identified in a study on congenital hydrocephalus (Shaheen et al., 2017). The heterotopia was shown to be undulating, resembling cortical architecture with gyri and sulci. In addition, the overlying cortex was noted to be malformed with a polymicrogyria-like appearance, the corpus callosum absent and 3/6 individuals described also had congenital hydrocephalus. All individuals were macrocephalic (>2.5 SD), and, even after intraventricular shunt drainage, the head circumference remained enlarged consistent with megalencephaly rather than simply hydrocephalus.

In this report, we provide further clinical and/or imaging details for the three previously published *EML1* families and describe two novel, unrelated individuals with a homozygous partial *EML1* deletion and a homozygous missense variant c.760G>A, p.(Val254Met), respectively. We show that the imaging phenotype associated with *EML1* mutations is consistent and the disorder can be recognized by the unique appearance on brain MRI. For one affected individual, we describe in great detail both the pre- and postnatal imaging characteristics and show that this syndrome can be recognized during pregnancy if monitored by fetal ultrasound and/or fetal MRI.

2 | METHODS

2.1 | Editorial policies and ethical considerations

The inclusion of the described individuals for research studies has been approved by the ethical committees of the respective institutions.

2.2 | Cohort recruitment and genetic testing

Clinical and imaging data from affected individuals belonging to five unrelated pedigrees, were collected through collaboration within the European Network on Brain Malformations (Neuro-MIG, COST Action CA16118; www.neuro-mig.org) and personal communication with the previous authors. Written informed consent for publication of photographs was obtained from parents/guardians by each physician. Family 1 was identified in the diagnostic setting. Families 2, 3, and 4 have been previously described (Kielar et al., 2014; Shaheen et al., 2017). Families 2 and 3 were originally recruited in research studies to reveal the genetic basis of MCD, Family 4 was recruited in a hydrocephalus study. For individual 8, exome sequencing of blood-derived DNA was performed using an Illumina NovaSeq system with subsequent targeted analysis of *EML1* with Agilent Alissa software.

3 | RESULTS

3.1 | Clinical reports

Clinical data are summarized Table 1.

Family 1. The proband is a three-year-old boy born by forceps-assisted vaginal delivery at 37 weeks of gestation following a pregnancy complicated by maternal syncope at 5 months during a period of fasting. Routine obstetric ultrasound at 20 weeks was reported as normal. He was the first child born to parents who are both of Lebanese origin and were not reported to be related. One of the maternal great nephews was reported to have a large head, but otherwise there was no relevant family history. His Apgar scores were 5 at 1 min and 7 at 5 min. He required CPAP for 72 hours due to respiratory distress and nasogastric feeding for 14 days. His birth head circumference was documented as 35 cm (50th centile) with weight 3.06 kg (25th centile) and length 47 cm (sixth centile).

Postnatally, cranial ultrasound at 7 days of age identified agenesis of the corpus callosum. Brain MRI at 8 days of life showed abnormalities as

TABLE 1 Characteristics of all affected individuals with *EML1* mutations

Patient ID	Family 1	Family 2	Family 2	Family 2	Family 3	Family 3	Family 4	Family 5
	Individual 1	Individual 2	Individual 3	Individual 4	Individual 5	Individual 6	Individual 7	Individual 8
Previous reference	NA	(Kielar et al., 2014) P135-3	(Kielar et al., 2014) P135-4	(Kielar et al., 2014) P135-5	(Kielar et al., 2014) 3489-4	(Kielar et al., 2014) 3489-5	(Shaheen et al., 2017) Family 22	NA
Gender	M	M	M	M	M		F	M
Age	3 years	22 years	24 years	NA	6 years	Fetus	2 years	8y
Ethnicity	Lebanese	Caucasian	Caucasian	Caucasian	Moroccan	Moroccan	Saudi Arabian	Pakistani
EML1 mutations *NM_004434.2*	Homozygous Exon 1 deletion: Arr[hg19] 14q32.2 (100,256,118-100, 271,376) x0matpat	Compound heterozygous c.412C>T; p.(Arg138*)	Compound heterozygous c.412C>T; p.(Arg138*)	Compound heterozygous c.412C>T; p.(Arg138*)	Homozygous c.673T>C; p.(Trp225Arg)	Homozygous c.673T>C; p.(Trp225Arg)	Homozygous c.1567C>T, p.(Arg523*)	Homozygous c.760G>A, p.(Val254Met)
		c.727A>G; p.(Thr243Ala)	c.727A>G; p.(Thr243Ala)	c.727A>G; p.(Thr243Ala)				
Birth measurements	OFC 50th centile, weight 25th centile, length sixth centile	OFC +2.5 SD	OFC +2.5 SD	OFC +2.5 SD	OFC +6 SD 1 week pp	NA	NA	OFC >> +2.5 D
Current height (cms/ *SD*)	98 cm	Normal	175 cms	NA	−5 SD (10 years)	NA	NA	NA
Current OFC (cms/ *SD*)	3 years: 57.5 (>99th centile, z = 5.41)	> 2 SD, and 2 SD at 10 years	>2 SD, and 2.5 SD at 2 years	+2.5 SD (1 years)	+3.3 SD (10 years)	NA	NA	NA
Milestones	Can briefly sit unsupported, no expressive speech	Ambulant	Ambulant	NA	No independent sitting or walking	NA	NA	NA
Cognition	Severe global DD	Severe ID, some words, some associations	Severe ID, some words, some associations	NA	No speech, profound ID	NA	Profound DD	Profound DD: Motor, visual, speech, social
Hydrocephalus	No	No	No	No	Yes, congenital	NA	Yes, congenital	Yes, congenital
Epilepsy	No	Refractory epilepsy (VNS, 4 AED), atonic, CGTC	Refractory epilepsy (VNS, 4 AED), atonic, CGTC	NA	Refractory epilepsy (3 AED), focal and GTC seizures	NA	Yes, intractable	Yes, onset 2y

(Continues)

TABLE 1 (Continued)

Patient ID	Family 1	Family 2	Family 2	Family 2	Family 3	Family 3	Family 4	Family 5
EEG	9 m: Absence of posterior dominant rhythms, frequent spike and wave discharges of parieto-occipital regions	NA	NA	NA	Epileptic encephalopathy and continuous multifocal epileptic discharges and frequent electrodecremental events accompanied by tonic seizures	NA	NA	NA
Muscle tone, movement	Axial hypotonia with appendicular hypertonia and brisk reflexes	Normal	Normal	NA	Axial hypotonia with hypertonia and pyramidal signs of extremtities, varus feet, bilateral adduction of the hips	NA	Hypotonia	Spastic tetraplegia, CK normal
Hearing	Normal	Normal	Normal	NA	NA	NA	NA	NA
Vision	Cortical visual impairment, right esotropia	Severe hypermetropia	Nystagmus and hypermetropia	NA	Bilateral convergent strabism and cortical visual impairment	NA	Strabismus and optic atrophy	Retinal dystrophy with retinal folds, rod and cone dysfunction
Miscellaneous	Small atrial septal defect				Gastric tube feeding, pectus carinatum	TOP due to prenatal ultrasound abnormalities		NG tube feeding

Abbreviations: AED = anti-epileptic drugs, DD = developmental delay, F = female, ID = intellectual disability, M = male, NA = not assessed, NG = nasogastric, SD = standard deviation, TOP = termination of pregnancy.

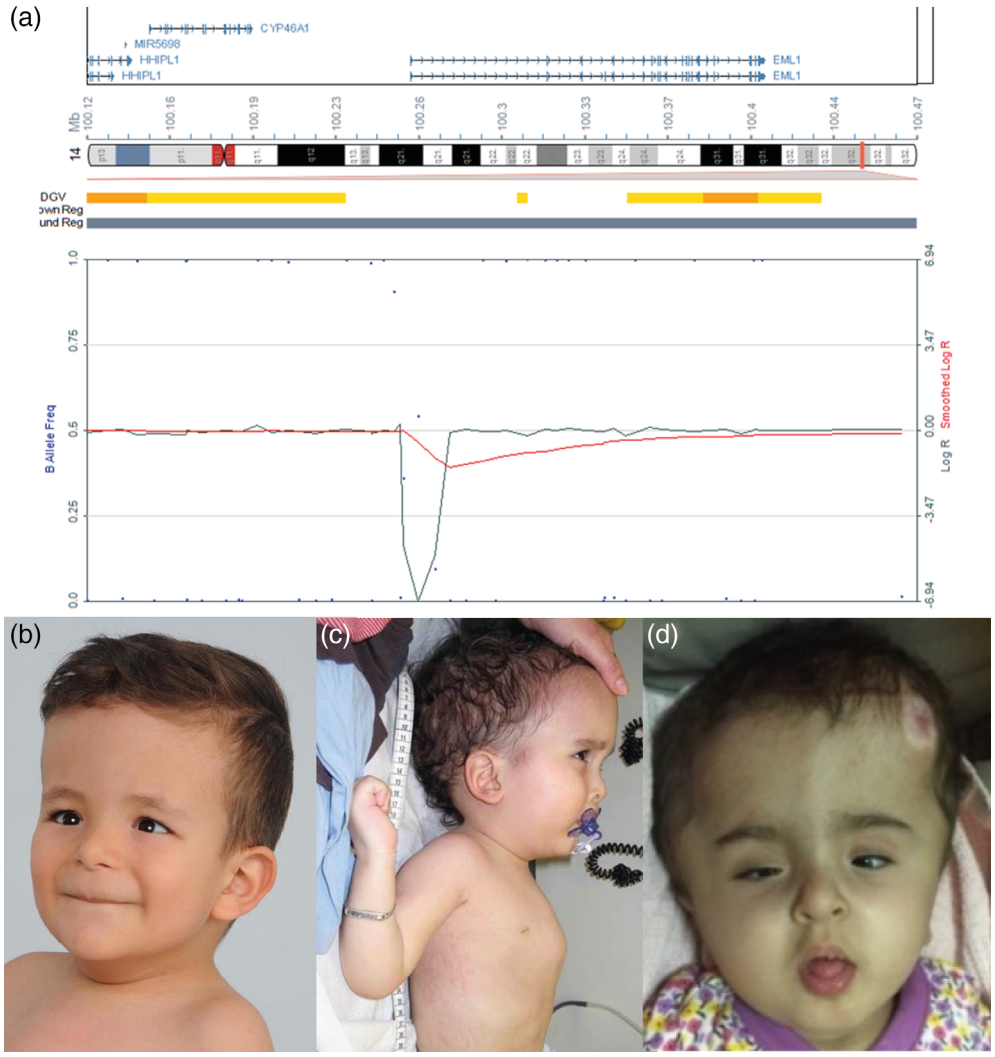

FIGURE 1 (a) Partial homozygous *EML1* deletion of Individual 1, screen shot of the SNP microarray IlluminaHumanOmni 2.5-8v1.2; 2,500 K result. (b) Facial photograph of Individual 1, depicting macrocephaly, high forehead, downslanting and narrow palpebral fissures, esotropia, a low-set left ear, long upper lip and a small chin. (c) Photograph of Individual 5. Note macrocephaly and prominent forehead, low-set ear, chest deformity, and abnormal posturing. (d) Facial photograph of Individual 7. Note macrocephaly, narrow palpebral fissure, esotropia and small mouth. This picture was previously published by Shaheen et al. [Reprinted with permission from John Wiley and Sons under license number 4562451107943]

described below. Cardiac ultrasound showed a small atrial septal defect and renal ultrasound was normal.

At age 39 days he was admitted to a tertiary pediatric hospital due to concerns regarding rapid head growth. His head circumference was 41 cm, having crossed from the 50th centile at birth to the 99th centile. Workup included CMV PCR and very long chain fatty acids, which were both normal.

SNP chromosome microarray (Illumina HumanCytoSNP-12 v2.1; 300 k) showed multiple long stretches of homozygosity (>2 Mb) on chromosomes 1, 2, 3, 5, 7, 8, 11, 13, 14, and 15 (4.1% of the genome) consistent with parental consanguinity. Within a region of homozygosity on chromosome 14, a homozygous deletion of approximately 0.2 Mb was identified at 14q32.2 and reported as arr[hg19] 14q32.2(100,256,118-100,271,376)x0matpat. The deletion resulted in loss of exon 1 of the canonical transcript of the *EML1* gene (NM_001008707). The homozygous deletion was confirmed on a second high-resolution SNP microarray platform (IlluminaHumanOmni 2.5-8v1.2; 2,500 K, Figure 1a). Parental microarrays confirmed that both parents are heterozygous carriers of the deletion (data not shown).

At age 37 months he was noted to have severe global developmental delay. He could roll and sit unsupported briefly but could not pull to stand or walk independently. He had no expressive language. He could pick up toys but could not feed himself. Audiology testing was normal. He had cortical visual impairment and a right esotropia. No seizures were reported. Physical examination showed a head circumference of 57.5 cm (>99th centile, z = 5.41), weight 17 kg (85th centile) and length 98 cm (44th centile). He had axial and appendicular hypotonia with normal strength and 1+ reflexes generally. Plantar responses were downgoing. He had a high forehead, slightly low set ears, prominent eyebrows with downslanting palpebral fissures, a small chin, a long upper lip, normal male genitalia, four small café au lait spots and incurving of the fifth toes. Facial photograph is shown in Figure 1b.

Family 2 has been described previously as family P135 (Kielar et al., 2014). We received information on two of the brothers, who are now adults with severe intellectual disability (ID), drug-resistant epilepsy, and macrocephaly. They did not have motor defects. Both had brain MRI in childhood but unfortunately images were not available for further review. In the previous publication ribbon-like

heterotopia, partial agenesis of the corpus callosum, enlarged ventricles and a polymicrogyria-like cortex were described. Compound heterozygous *EML1* variants were identified: c.481C>T; p. (Arg138*) and c.796A>G; p.(Thr243Ala).

Family 3 has been described previously as family 3,489 (Kielar et al., 2014). The index patient presented prenatally with ultrasound abnormalities. His parents were consanguineous and of Moroccan descent. They had had one miscarriage, and a termination of pregnancy after signs of similar features on fetal ultrasound at 20 GW. The proband was born at 33 weeks and 3 days of gestation by caesarean section for progressive hydrocephalus on ultrasound examinations. A ventriculo-peritoneal shunt was inserted after birth. At age 6 years he had profound ID and became wheelchair bound. He had a responsive smile and could roll over. He frequently aspirated on liquids and was unable to eat solid foods. He had short stature (−4 *SD*) and was macrocephalic (+3.3 *SD*). He had severe cortical visual impairment with absence of visual tracking. EEG at age 7, while taking levetiracteam and valproic acid, was consistent with an epileptic

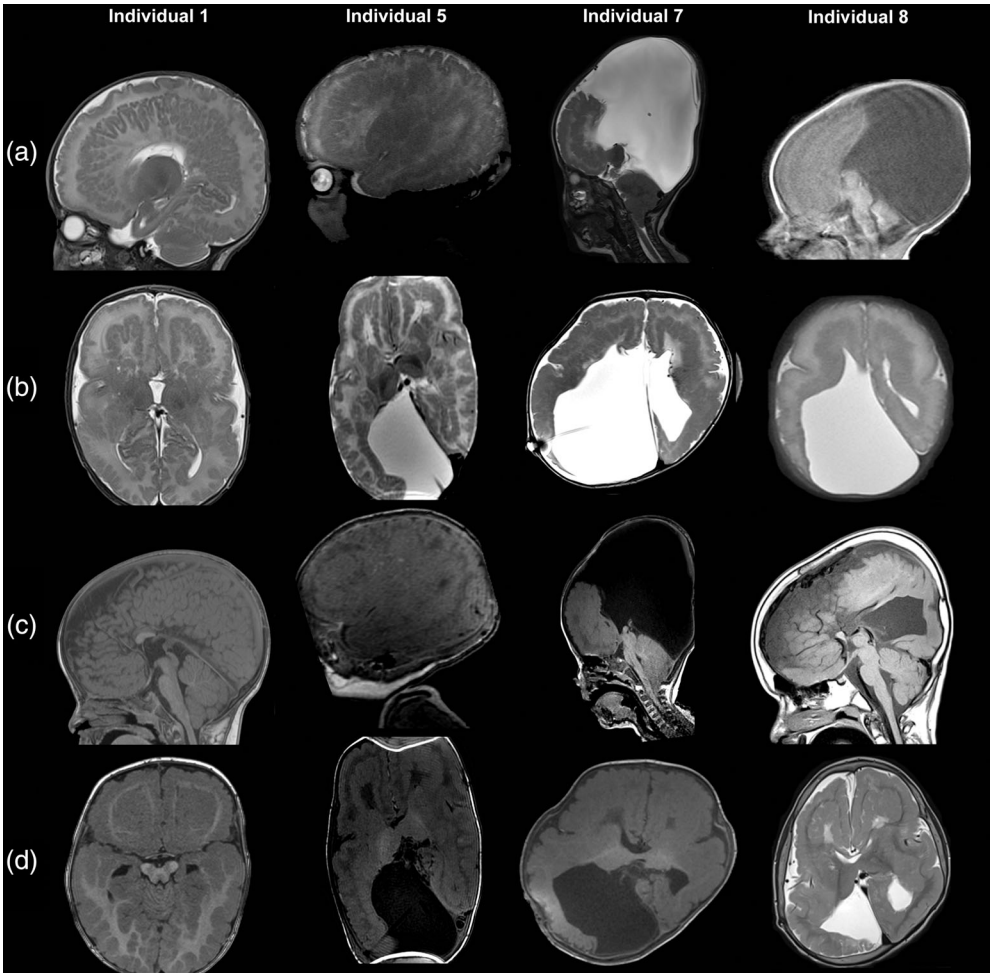

FIGURE 2 Brain MR imaging of Individuals 1, 5, 7, and 8. Individual 1 a-b: Sagittal and axial T2 scans at 39 days of life demonstrates thin cortex with shallow polygyria; symmetrical undulating ribbon-like heterotopia is also noted in the subcortical region. (c, d) Axial and sagittal T1 weighted scans at age 13 months demonstrate myelinated white matter on both sides of the ribbon-like heterotopia in the periventricular regions and the subcortical regions. The sagittal T1 midline image (a) at 13 months shows further head growth with bossing of forehead. The corpus callosum is hypoplastic. There is progression of myelination and development of macrocerebellum with large vermis and ectopic cerebellar tonsils. The pons is flat and the midbrain is short. Individual 5 a-d: Sagittal and axial T2 (a, b) and T1 (c, d) weighted images obtained at 4 months of age show the same typical ribbon-like heterotopia with overlying polymicrogyric cortex. There is frontal bossing and an enlarged right occipital horn. Note the medial fusion of small and rotated thalami (b, d). On the sagittal T1 (c) high signal areas are visible, which are low on T2. Individual 7 A-D: Sagittal and axial T2 (a, b) and T1 (c, d) weighted images at age 11 months show macrocephaly with extreme enlargement of the occipital horns, right more than left with compression on the tentorium and posterior fossa with tonsillar herniation through foramen magnum. The ribbon-like heterotopia and abnormal dysgyric overlying cortex are seen in all lobes. Note also the medial fusion of the dysmorphic thalami (d). Partial callosal agenesis with presence of a very thin rostrum and genu was noted. Individual 8 a-d: Sagittal T1 (a, c) and axial T2 (b, d) weighted images at age 5 days (a, b) and 8 years (c, d). Note the large interhemispheric cyst communicating with the occipital horn of the right lateral ventricle (a, b), partial agenesis of the corpus callosum (a, c). Postnatally, the thin dysplastic cortex with shallow sulci and the ribbon-like heterotopia is easily noted (b). The basal ganglia are severely hypoplastic and the thalami are fused (d). Note also the patchy white matter changes especially in the frontal lobes (d)

encephalopathy showing continuous multifocal epileptic discharges and frequent tonic seizures accompanied by an electrodecremental response. Whole-exome-sequencing showed a homozygous *EML1* variant c.673T>C; p.(Trp225Arg). The fetus was, after termination of pregnancy, also found to be homozygous for the *EML1* variant but was not further examined.

Family 4 was previously described as family 22 (Shaheen et al., 2017) and brief clinical details were published in the supplements. A facial photograph of the affected girl is reprinted with permission and shown in Figure 1d. The mother of the index patient presented in her seventh pregnancy. Fetal hydrocephalus was identified necessitating Caesarean Section at 35 GW. Congenital hydrocephalus was managed with a ventriculoperitoneal shunt but the child developed drug-resistant epilepsy and profound global developmental delay. The parents were first cousins and lost a daughter previously with similar clinical and imaging features (no genetic testing). Physical examination revealed macrocephaly, deformational plagiocephaly, and hypotonia. Ophthalmological assessment showed strabismus and optic atrophy. A homozygous *EML1* nonsense variant was identified through exome sequencing: c.1567C>T, p.(Arg523*).

Family 5. The proband (Individual 8) was born to consanguineous parents of Pakistani descent, prematurely at 32 GW. He was diagnosed with congenital hydrocephalus subsequently treated with ventriculoperitoneal shunt. He started having seizures at age 2 years that were controlled with vigabatrin initially, followed by sodium valproate. However recently, he has been referred back to neurosurgery with worsening seizures. His development was noted to be severely delayed, at current age he is wheelchair dependent with spastic tetraplegia and he fed through a nastrogastric tube. He was also diagnosed with panretinal dystrophy and is registered blind. Exome sequencing with targeted analysis of *EML1* revealed a nonsynonymous homozygous variant NM_004434.2 c.760G>A, p.(Val254Met). Parental DNA samples were not available. The variant was absent in the GnomAD database. In silico predictions showed a probably pathogenic effect; SIFT: deleterious; MutationTaster: disease-causing; PolyPhen2: probably damaging.

3.2 | Imaging review

The key imaging features of all *EML1* patients are generalized megalencephaly, periventricular and ribbon-like subcortical heterotopia, partial or total callosal agenesis, and a polymicrogyria-like cortical malformation (see Figure 2). The heterotopia are located in the region of the outer subventricular zone and form a rudimentary sulcal/gyral pattern resembling a second inner cortex. For Individual 5 fetal ultrasound was performed at 17 and 24 weeks and a fetal MRI at 22 weeks gestation. Postnatally, MRI was performed on day 1, 3 months and 3 years and 9 months (Figures 2 and 3). The fetal ultrasounds showed features of callosal agenesis and congenital hydrocephalus. The fetal MRI confirmed the callosal agenesis and abnormal configuration of the lateral ventricle with interhemispheric extension and suspicion of an extensive migration disorder. The aspect of the heterotopia appears to change in time, prenatally and even postnatally, resulting in increased folding and thickening of the heterotopic layer. The overlying cortex is abnormal with a polymicrogyria-like appearance, with a "lumpy-bumpy" inner and outer surface though the gyri and sulci are overall shallow. Similar to subcortical band heterotopia, normally myelinating white matter is present in between the cortex and the heterotopic gray matter. The folding of the brain surface may be masked by co-occuring hydrocephalus if present, making it difficult to assess the extent of the abnormally formed cortex, especially on fetal ultrasound. After ventricular shunting,

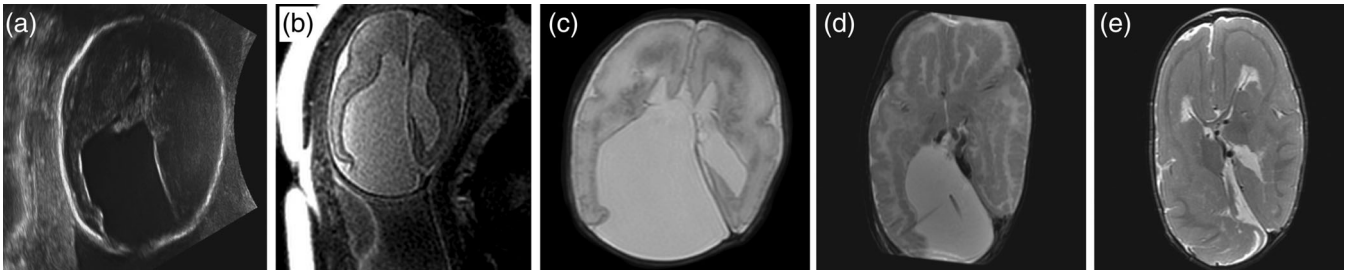

FIGURE 3 Imaging pattern at different ages. Prenatal ultrasound at 17 weeks of gestational age (a), prenatal MRI at 22 weeks gestational age (b), postnatal MRI at birth (c), at 3 months (d) and at 3 years and 9 months (e) of affected individual 5. Fetal ultrasound at 17 weeks shows a posterior interhemispheric cyst communicating with an enlarged right occipital horn (a). On follow-up ultrasound, not shown, the dilation of the lateral ventricles increased. Even on the earliest ultrasound the ribbon-like band heterotopia is visible at the ventricular border, though not fully recognized at that time. Also the overlaying cortex seems abnormal. Fetal MRI at 22 weeks (b): The T2 weighted image is in line with the previous ultrasound findings. The macrocephaly with the colpocephaly of the right occipital horn with extention into the posterior part of the interhemispheric space can be delineated. The periventricular migration disturbance is visible in both cerebral hemispheres, which already shows its ribbon-like appearance. Postnatal MRI at the day of birth at 33 weeks and 3 days (c): This axial T2 weighted image shows the ribbon-like heterotopia similar to the fetal MRI. The abnormal cortex is better visualized here. Periventricular T1 high signal areasare noted. MRI at 4 months of age (d) shows a clearer picture of the ribbon-like band heterotopia. The heterotopia is thicker compared to the MRI at birth (c) and the overlying cortex shows a more clear "lumpy bumpy" appearance. The right occipital horn is slightly decreased in size after ventriculo-peritoneal drain placement visible on this axial T2 weighted image. At 3 years and 9 months a follow-up MRI (e) shows further thickening of the heterotopia which occupies a large part of white matter space. Note the unchanged abnormal appearance of the thalami and basal ganglia

the abnormal appearance of the cortex remains and the overgrowth of the supratentorial brain parenchyma continues resulting in megalencephaly and rapid growth of the skull vault. This overgrowth is seen in all patients, independent of the presence of congenital hydrocephalus. The basal ganglia are usually hypoplastic and the thalami may be fused. The anterior limb of the internal capsule is normally formed. All cases showed partial or complete callosal agenesis.

In two patients focal T1 hyperintensities were visible in the region of the outer subventricular zone, which could be calcifications, small hemorrhages or gliosis, (see Figure 2 sagittal T1 of Individual 5) but not specific in nature.

4 | DISCUSSION

From review of the clinical and imaging data of eight individuals from five families with biallelic *EML1* mutations a unique phenotype emerges. This syndrome is characterized by severe developmental delay, often drug-resistant seizures, visual impairment, and macrocephaly. On brain imaging there is megalencephaly with a very characteristic ribbon-like heterotopia, combined with partial or complete callosal agenesis and an overlying polymicrogyria-like cortex. Several of these features can be recognized on prenatal imaging. Review of sequential imaging performed for Individual 5 illustrates that several of these imaging features, especially the abnormally formed lateral ventricles, hydrocephalus if present and - suspicion of—a cortical malformation, can be detected during third trimester using fetal MRI and even prenatal ultrasound. This may allow for the provision of a prenatal diagnosis and accurate genetic counseling of the parents, although the features may not be identified until late in the pregnancy when intervention or timely genetic testing may not be possible. Another interesting observation is that the appearance of the heterotopia changes over time, and seems to progressively occupy more of the subcortical space. As stated by Barkovich in 2003, migrational disorders like polymicrogyria may change over time (Takanashi & Barkovich, 2003). They reviewed a case for which the polymicrogyria changed from pattern 1 (small, fine, and undulating cortex with normal thickness (3–4 mm) to pattern 2, a bumpy cortex that appeared abnormally thick (6–8 mm) and had an irregular cortical–white matter junction. They postulated that the myelination of the intracortical and subcortical fibers causes changes in the appearance and apparent thickness of the polymicrogyric cortex on T2-weighted images. In *EML1*-associated cases, the heterotopia is located in the outer subventricular zone. In time, this zone thickens from a small undulating line of cells on the fetal and neonatal scans to thickening of this zone to near 10 mm. It remains speculative which cell type is responsible for this change. The subcortical white matter zone (visible as a myelinated small zone) is outside of this thickened subventricular zone, so we hypothesize that the thickening is not due to changes in the intracortical or subcortical white matter fibers in the *EML1* cases. Besides this thickening, there is also an increase in gyration of the overlying cortex. This is also part of normal aging but might in part be influenced by the underlying thickened layer of heterotopic cells at the outer subventricular zone.

4.1 | Molecular genetics

Both loss-of-function and missense mutations were observed. All three missense mutations cluster in the HELP motif (amino acids 217–259). The HELP motif is a characteristic and conserved hydrophobic component of the EML protein family (Richards et al., 2014) and is in EML1 part of the TAPE domain, required for tubulin binding (Richards et al., 2014). In vitro studies have shown that the Thr243Ala mutation indeed impairs the association of Eml1 with microtubules (Kielar et al., 2014).

No clear genotype–phenotype correlation emerges and both individuals with homozygous missense as well as nonsense variants have a severe clinical presentation. This suggests that the missense variants also negatively impact protein function. The affected individuals from Families 1 and 2 lack hydrocephalus, and epilepsy is absent up to the age of 3. In addition, the individuals from Family 2 had no motor impairment, in stark contrast to the severe motor delay observed in the others. It would be interesting to study the effect at the protein level of the mutations, especially that of the exon 1 deletion. Alternative start codons downstream of the protein might allow EML1 protein expression. On the other hand, complete loss of EML1 expression is also expected for Individual 7 with the homozygous p.(Arg523*) variant.

Another patient with *EML1*-like brain abnormalities has been described (Nagaraj, Hopkin, Schapiro, & Kline-Fath, 2017). After publication of this report, compound heterozygous *EML1* variants; c.1316G>A (p.Gly439Asp) and c.1433G>T p.Gly478Val) have also been identified in this individual (personal communication Usha Nagaraj). This finding confirms the highly specific pattern of brain abnormalities associated with *EML1* pathogenic variants.

4.2 | Differential diagnosis

Syndromes with overlapping features that could be considered in the differential diagnosis are shown in Table 2. The case published by Kobayashi et al also shows striking resemblance to the *EML1* phenotype (Kobayashi et al., 2016). They describe a girl with progressive megalencephaly, drug-resistant seizures and severe developmental delay. On MRI bilateral symmetrical polymicrogyria predominantly in the perisylvian to posterior regions, and extensive symmetrical heterotopia in the periventricular region with posterior-temporal dominance was noted. The corpus callosum was present, but hypoplastic. Similar to the *EML1*-patients, the heterotopia form a continuous undulating band.

The imaging pattern also shows overlap with that observed in the Chudley McCullough syndrome. In these individuals subcortical heterotopia, agenesis/hypogenesis of the corpus callosum, and ventriculomegaly are frequently present (Doherty et al., 2012). Although they can have macrocephaly and seizures, clinically they present differently with hearing loss, and absent or only mild ID in stark contrast to the severe ID observed in the *EML1* patients (Doherty et al., 2012). Moreover, the subcortical heterotopia is either

TABLE 2 Review of syndromes with similar heterotopia

	EML1- related ribbon-like heterotopia	Chudley McCullough s yndrome	Parrini et al., 2006	Tsuburaya et al., 2012	Kobayashi et al., 2016
Gene	*EML1*	*GPSM2*	Unknown 2 individuals	Unknown 1 individual	Unknown 1 individual
Inheritance	Autosomal recessive	Autosomal recessive	Unknown	Unknown	Unknown
Clinical features					
Development	Severe ID	Normal- mild ID	Normal	Severe DD	Severe DD
Epilepsy	+, severe	+, infrequent	+	+, severe	+, severe
Head size	Macrocephaly	Macrocephaly	Unknown	Acquired microcephaly	Macrocephaly
Other		Sensorineural hearing loss		Congenital cataract	Regression with loss of skills
Imaging features					
Heterotopia	Subcortical	Subcortical frontal–parietal heterotopia, parallel to cingulate gyri, can be small nodular, or form a larger irregular band	Ribbon-like heterotopia encircling the posterior Bodies and occipital horns of the lateral ventricles	Ribbon-like heterotopia, Encircling from the body to the posterior horns the lateral ventricles	Symmetrical Heterotopia in the periventricular region with Posterior-temporal dominance
Cortex	Generalized PMG-like cortex	Frontal PMG	Normal	Simplified gyral pattern	Bilateral PMG predominantly in the perisylvian to posterior regions
Ventricles	Ventriculomegaly-hydrocephalus	Non-obstructive, asymmetric ventriculomegaly	Normal	Ventriculomegaly	Normal
Corpus callosum	Complete agenesis	Partial –complete agenesis	Normal	Partial agenesis	Hypoplasia
Cerebellum		Dysplasia	Normal	Possible hypoplasia	Normal
Other		Arachnoid cysts		Arachnoid cyst, delayed myelination	

Abbreviations: DD, developmental delay; ID, intellectual disability; PMG, polymicrogyria.

not or only slightly festooned and not as diffuse as in *EML1* mutations, and shows a predilection for the cingulate gyrus.

Ribbon-like heterotopia have also been described in other patients as being located more closely to the lateral ventricles (Parrini et al., 2006; Tsuburaya et al., 2012). These heterotopia showed a strong sinusoidal morphology. We have found descriptions of three unrelated individuals, two with normal cognition and childhood onset epilepsy, and one with severe developmental delay, drug-resistant epilepsy, microcephaly and cataracts (Parrini et al., 2006; Tsuburaya et al., 2012).

4.3 | Mechanism

EML1 encodes a microtubule-associated protein. Microtubules play an important role in several stages of cortical development, including neurogenesis, migration, and organization (Breuss, Leca, Gstrein, Hansen, & Keays, 2017). It is therefore not surprising that mutations in many genes encoding microtubule components and microtubule-associated proteins have already been associated with MCD, for example the major lissencephaly genes *DCX* and *PAFAH1B1* (also known as *LIS1*), and the tubulin genes associated with the complex malformations of the tubulinopathies (Bahi-Buisson & Cavallin, 1993; Di Donato et al., 2018). Interestingly, certain disorders are associated with microcephaly, which may be caused by mitotic errors leading to cell cycle arrest and/or apoptosis, causing a depletion of the progenitor or neuronal pool (Alcantara & O'Driscoll, 2014). Instead, *EML1* mutations lead to the opposite phenotype of megalencephaly.

Most knowledge on the role of *EML1* in brain development comes from studies on the *HeCo* mouse mutant. This spontaneous *Eml1* mutant shows ectopic proliferating cells in the intermediate zone (IZ) and cortical plate (CP) at E13 and develops subcortical heterotopia (Kielar et al., 2014). An increased labeling index and reduced cell cycle exit was observed. Mutant cells in the VZ at E13.5 have longer mitotic spindles and an abnormal cell shape, in addition to centrosome and cilia defects (Bizzotto et al., 2017; Uzquiano et al., 2019). It is hypothesized that these altered cellular dynamics lead to delamination, with Radial Glial Cells (RGCs) being pushed out of the VZ while maintaining their proliferative capacity (Bizzotto et al., 2017). RGCs are essential to neuronal proliferation and migration as they can give birth to neurons by asymmetric cell division or indirect neurogenesis, and they provide a scaffold for newborn neurons migrating toward the cortical plate (Jiang & Nardelli, 2015). The neurons do not lose their normal migrating capacities, but many cells remained sequestered in the heterotopia, due to local neuron production in the IZ and alteration of the radial glial cell migration guides (Kielar et al., 2014). Interestingly, the GPSM2 (a.k.a. LGN) mouse model also demonstrates increased numbers of neural progenitor cells proliferating in ectopic locations throughout the cortical wall (Konno et al., 2008). Altered spindle orientations, also observed in the *HeCo* mouse, have been highlighted as a mechanism leading to delaminated radial glia progenitors. Further mouse mutants with ectopic progenitors have also been described (Romero, Bahi-Buisson, & Francis, 2018).

Hydrocephalus is not observed in every case of *EML1* mutation. Genetic background effects may contribute to this outcome. In a new *Eml1* knockout mouse model on the C57BL/6 background, postnatal hydrocephalus was also observed in some mice, but not all, and this phenotype was not originally observed in the HeCo model on the NOR/CD1 background (Collins et al., 2019; Kielar et al., 2014). Recently, it has been shown that mutations in *Eml1*/*EML1*, found in mice and patients with subcortical heterotopia, impair primary cilia formation in apical progenitors (Uzquiano et al., 2019). Ciliopathies, for example Meckel-Gruber and hydrolethalus syndrome, show a high incidence of congenital hydrocephalus (Parisi & Glass, 1993). In a mouse model, it was shown that depletion of the primary cilium in radial glial cells lead to prenatal ventriculomegaly, which was associated with an increase in size of the RGC apical domain and an activation of the mTOR pathway (Foerster et al., 2017). This suggests that primary cilia defects can directly influence the morphology of the ependyma. In addition, altered mTOR signaling may contribute to the overgrowth of the brain and the ribbon-like, "pseudo cortex" appearance, and characteristic for this mutation. Further work is required to study this mechanism in *Eml1* mouse mutants.

5 | CONCLUSION

In conclusion, truncating variants and missense variants clustering in the HELP motif in *EML1* lead to a recognizable syndrome characterized by severe developmental delay, drug-resistant seizures and visual impairment. On brain imaging there is megalencephaly with a characteristic ribbon-like subcortical heterotopia, combined with partial or complete callosal agenesis and an overlying polymicrogyria-like cortical malformation. In addition, several individuals were diagnosed with congenital hydrocephalus. EML1 function can be related to microtubules and primary cilia, which again emphasizes their important role in brain and especially cortical development.

ACKNOWLEDGMENTS

We thank the families described herein for their collaboration. We also thank Fowzan Alkuraya and Ranad Shaheen (King Faisal Specialist Hospital and Research Center, Riyadh, Saudi Arabia) for sharing the imaging of Individual 7. Roy Sanders (UMC Utrecht) has helped with drafting the figures. FF is associated with the BioPsy Labex project and the Ecole des Neurosciences de Paris Ile-de-France (ENP) network, supported by Inserm, Centre national de la recherche scientifique (CNRS), Sorbonne Université, the JTC 2015 Neurodevelopmental Disorders affiliated with the ANR (for NEURON8-Full-815-006 STEM-MCD, to FF, NBB) and the Fondation Maladies Rares/Phenomin (project IR4995, FF).

CONFLICT OF INTEREST

The authors have no conflict of interest to declare.

ORCID

Renske Oegema https://orcid.org/0000-0002-7146-617X
Grazia M. S. Mancini https://orcid.org/0000-0002-1211-9979

REFERENCES

Alcantara, D., & O'Driscoll, M. (2014). Congenital microcephaly. *American Journal of Medical Genetics. Part C, Seminars in Medical Genetics*, *166C* (2), 124–139. https://doi.org/10.1002/ajmg.c.31397

Bahi-Buisson, N., & Cavallin, M. (1993). Tubulinopathies overview. In M. P. Adam, H. H. Ardinger, R. A. Pagon, S. E. Wallace, L. J. H. Bean, K. Stephens, & A. Amemiya (Eds.), *GeneReviews*. Seattle (WA): University of Washington.

Bizzotto, S., Uzquiano, A., Dingli, F., Ershov, D., Houllier, A., Arras, G., … Francis, F. (2017). Eml1 loss impairs apical progenitor spindle length and soma shape in the developing cerebral cortex. *Scientific Reports*, *7* (1), 17308. https://doi.org/10.1038/s41598-017-15253-4

Breuss, M. W., Leca, I., Gstrein, T., Hansen, A. H., & Keays, D. A. (2017). Tubulins and brain development - the origins of functional specification. *Molecular and Cellular Neurosciences*, *84*, 58–67. https://doi.org/10.1016/j.mcn.2017.03.002

Collins, S. C., Uzquiano, A., Selloum, M., Wendling, O., Gaborit, M., Osipenko, M., … Francis, F. (2019). The neuroanatomy of Eml1 knockout mice, a model of subcortical heterotopia. *Journal of Anatomy*, *235* (3), 637–650. https://doi.org/10.1111/joa.13013

Di Donato, N., Timms, A. E., Aldinger, K. A., Mirzaa, G. M., Bennett, J. T., Collins, S., … Dobyns, W. B. (2018). Analysis of 17 genes detects mutations in 81% of 811 patients with lissencephaly. *Genetics in Medicine*, *20*(11), 1354–1364. https://doi.org/10.1038/gim.2018.8

Doherty, D., Chudley, A. E., Coghlan, G., Ishak, G. E., Innes, A. M., Lemire, E. G., … Zelinski, T. (2012). GPSM2 mutations cause the brain malformations and hearing loss in Chudley-McCullough syndrome. *American Journal of Human Genetics*, *90*(6), 1088–1093. https://doi.org/10.1016/j.ajhg.2012.04.008

Foerster, P., Daclin, M., Asm, S., Faucourt, M., Boletta, A., Genovesio, A., & Spassky, N. (2017). mTORC1 signaling and primary cilia are required for brain ventricle morphogenesis. *Development*, *144*(2), 201–210. https://doi.org/10.1242/dev.138271

Jiang, X., & Nardelli, J. (2015). Cellular and molecular introduction to brain development. *Neurobiology of Disease*, *92*, 3–17. https://doi.org/10.1016/j.nbd.2015.07.007

Kielar, M., Tuy, F. P., Bizzotto, S., Lebrand, C., de Juan Romero, C., Poirier, K., … Francis, F. (2014). Mutations in Eml1 lead to ectopic progenitors and neuronal heterotopia in mouse and human. *Nature Neuroscience*, *17*(7), 923–933. https://doi.org/10.1038/nn.3729

Kobayashi, Y., Magara, S., Okazaki, K., Komatsubara, T., Saitsu, H., Matsumoto, N., … Tohyama, J. (2016). Megalencephaly, polymicrogyria and ribbon-like band heterotopia: A new cortical malformation. *Brain Dev*, *38*(10), 950–953. https://doi.org/10.1016/j.braindev.2016.06.004

Konno, D., Shioi, G., Shitamukai, A., Mori, A., Kiyonari, H., Miyata, T., & Matsuzaki, F. (2008). Neuroepithelial progenitors undergo LGN-dependent planar divisions to maintain self-renewability during mammalian neurogenesis. *Nature Cell Biology*, *10*(1), 93–101. doi: ncb1673 [pii]. https://doi.org/10.1038/ncb1673

Nagaraj, U. D., Hopkin, R., Schapiro, M., & Kline-Fath, B. (2017). Prenatal and postnatal evaluation of polymicrogyria with band heterotopia. *Radiology Case Reports*, *12*(3), 602–605. https://doi.org/10.1016/j.radcr.2017.04.007

Parisi, M., & Glass, I. (1993). Joubert Syndrome. In M. P. Adam, H. H. Ardinger, R. A. Pagon, S. E. Wallace, L. J. H. Bean, K. Stephens, & A. Amemiya (Eds.), *GeneReviews*. Seattle, WA: University of Washington.

Parrini, E., Ramazzotti, A., Dobyns, W. B., Mei, D., Moro, F., Veggiotti, P., … Guerrini, R. (2006). Periventricular heterotopia: Phenotypic heterogeneity and correlation with Filamin a mutations. *Brain*, *129*(Pt 7), 1892–1906. https://doi.org/10.1093/brain/awl125

Richards, M. W., Law, E. W., Rennalls, L. P., Busacca, S., O'Regan, L., Fry, A. M., … Bayliss, R. (2014). Crystal structure of EML1 reveals the basis for Hsp90 dependence of oncogenic EML4-ALK by disruption of an atypical beta-propeller domain. *Proceedings of the National Academy of Sciences of the United States of America*, *111*(14), 5195–5200. https://doi.org/10.1073/pnas.1322892111

Romero, D. M., Bahi-Buisson, N., & Francis, F. (2018). Genetics and mechanisms leading to human cortical malformations. *Seminars in Cell & Developmental Biology*, *76*, 33–75. https://doi.org/10.1016/j.semcdb.2017.09.031

Shaheen, R., Sebai, M. A., Patel, N., Ewida, N., Kurdi, W., Altweijri, I., … Alkuraya, F. S. (2017). The genetic landscape of familial congenital hydrocephalus. *Annals of Neurology*, *81*(6), 890–897. https://doi.org/10.1002/ana.24964

Takanashi, J., & Barkovich, A. J. (2003). The changing MR imaging appearance of polymicrogyria: A consequence of myelination. *AJNR. American Journal of Neuroradiology*, *24*(5), 788–793.

Tsuburaya, R., Uematsu, M., Kikuchi, A., Hino-Fukuyo, N., Kunishima, S., Kato, M., … Tsuchiya, S. (2012). Unusual ribbon-like periventricular heterotopia with congenital cataracts in a Japanese girl. *American Journal of Medical Genetics. Part A*, *158A*(3), 674–677. https://doi.org/10.1002/ajmg.a.34258

Uzquiano, A., Cifuentes-Diaz, C., Jabali, A., Romero, D. M., Houllier, A., Dingli, F., … Francis, F. (2019). Mutations in the heterotopia gene Eml1/EML1 severely disrupt the formation of primary cilia. *Cell Reports*, *28*(6), 1596–1611 e1510. https://doi.org/10.1016/j.celrep.2019.06.096

How to cite this article: Oegema R, McGillivray G, Leventer R, et al. *EML1*-associated brain overgrowth syndrome with ribbon-like heterotopia. *Am J Med Genet Part C*. 2019; 181C:627–637. https://doi.org/10.1002/ajmg.c.31751